Clinical Biomechanics 27 (2012) 861–865

Contents lists available at SciVerse ScienceDirect

Clinical Biomechanics

journal homepage: www.elsevier.com/locate/clinbiomech

Damping properties of the nucleus pulposus

Arne Vogel, Dominique P. Pioletti *

Laboratory of Biomechanical Orthopedics, EPFL, Lausanne, Switzerland

ARTICLE INFO

Article history:
Received 17 January 2012
Accepted 6 June 2012

Keywords:
Dissipation
Damping
Hysteresis
Nucleus pulposus
Large deformation

ABSTRACT

Background: The nucleus pulposus is extremely deformable and it is not uncommon to observe strain amplitudes as large as 12.5% in physiological loading conditions. It has been shown that the nucleus pulposus contributes to the damping properties of the intervertebral disc. The quantification of the damping properties of the nucleus pulposus under physiological large deformations is then a key aspect for its mechanical characterization and for the design of nucleus replacement devices.
Methods: A specific mechanical device has been developed to encapsulate nucleus pulposus tissues into a deformable and permeable device, while quantifying its water content. The specific damping capacity was defined by dividing the energy loss by the work input. With this device and definition, the specific damping capacity of the bovine coccygeal nucleus pulposus was quantified in large compressive deformations (12.5%) and for frequencies ranging between 10^{-2} and 10^{1} Hz.
Findings: It is found that the specific damping capacity of the nucleus pulposus of the bovine coccygeal ranged between 18 and 36%. The lowest values of specific damping capacity are found for frequencies corresponding to the dynamics of loads in all day activities such as walking (0.1 to 1 Hz).
Interpretation: The nucleus pulposus contributes to dissipate energy under physiological large deformations. However, it seems that the nucleus pulposus is designed so that damping is minimal for frequencies corresponding to moderate daily activities.

1. Introduction

The intervertebral disc (IVD) is a complex joint that can bear important loads while allowing flexibility of the spine (Adams et al., 2006). The nucleus pulposus (NP) is a viscous gelatinous structure composed of a loose and random collagen fibril mesh embedded in a highly hydrated extrafibrillar network. It occupies approximately 50% of the IVD volume (Rannou et al., 2004).

The function of the NP in the biomechanics of the spine is essential. Indeed, the biomechanical function of the joint depends on the cooperative interaction between its structural components. Similar to a pneumatic system, the IVD can bear large compressive loads as the NP pressurizes and transfers the load to the bulging annulus fibrosus and cartilaginous endplates (Adams et al., 2006). The physiological loading condition of a NP could then be seen as a semi-confined situation. The NP is extremely deformable and it is not uncommon to observe strain amplitudes as large as 12.5% in physiological loading conditions (Tsantrizos et al., 2005). In parallel to its remarkable deformation property, in vivo experiments on baboon showed that removing the NP decreases the damping properties of the IVD (Quandieu et al., 1983). Therefore, it seems that, from a biomechanical standpoint, the NP has two main functions: a hydrostatic function to transfer the load to the surrounding tissues, and a viscous function to dissipate mechanical energy. In particular, it is believed that the central region of the IVD, comprising the inner annulus fibrosus and the nucleus pulposus, plays an important role in the damping properties of the IVD (Holzapfel et al., 2005; Iatridis et al., 1997; Leahy and Hukins, 2001).

In contrast to elastic properties of the NP, which have been well documented in the literature (Aladin et al., 2010; Boxberger et al., 2009; Cloyd et al., 2007; Perie et al., 2005), the viscous properties of the NP are far less studied with the exception of some works (Boxberger et al., 2009; Iatridis et al., 1997; Leahy and Hukins, 2001). In particular at large dynamic physiological strains and in unconfined or semi-confined situations, there is virtually no information on the damping properties of the NP. As a result, elastic aspects alone are generally considered for the design of nucleus replacement devices regardless the evidences that were reported for the damping contributions of the NP.

The objective of the present study is to introduce a semi-confined method to address the damping properties of nucleus pulposus under physiological deformations. In particular, the specific damping capacity of the coccygeal bovine nucleus pulposus was evaluated.

2. Methods

2.1. Study design

Nucleus pulposus damping properties were evaluated at different frequencies with a specifically semi-confined technique consisting in a PDMS chamber in which the NP can freely swell. To correct for the

* Corresponding author at: EPFL/STI/IBI/LBO, Station 19, 1015 Lausanne, Switzerland.
E-mail address: dominique.pioletti@epfl.ch (D.P. Pioletti).

0268-0033/$ – see front matter © 2012 Elsevier Ltd. All rights reserved.
doi:10.1016/j.clinbiomech.2012.06.005

damping properties cause by the PDMS chamber, damping properties were quantified for all the chambers (defined as control) and subtracted from the corresponding measurement performed with the NP. A specific damping metric was used allowing for this correction to be performed.

2.2. Specimen preparation

Six tails from 12 month old bovine were acquired from the local slaughterhouse. The NP of the largest coccygeal disc was excised in the axial direction using a 7 mm diameter biopsy punch (Fig. 1a,b). The NP samples were weighed and kept frozen at −18 °C within 12 h of slaughter. Twelve hours prior to testing, the NP samples were placed into a hydrogel encapsulation device (HED) and let to swell in a phosphate buffered saline (PBS) solution in the refrigerator at 4 °C (Izambert et al., 2003). The encapsulation device is composed of a medical grade 40 μm pore size sintered steel filter, a non-porous rigid disc, and a 100 μm thin polydimethylsiloxane (Sylgard 184, Dow Corning, USA) elastomer deformable membrane (Fig. 1c). Prior to testing, the samples were placed at room temperature (21 °C) for 3 h.

2.3. Dynamic compression testing

The samples were tested on a standard tension machine (Electropulse E3000, Instron, USA), equipped with specially designed fixtures (Fig. 2, left). These fixtures firmly grip the encapsulation device and force PBS through the device's porous filters to maintain the sample hydrated and at a temperature of 21 °C at all time. An initial 2 kPa pressure was applied and was used to define a reference configuration. Tests were then performed in sinusoidal strain amplitude control mode reaching a total of 12.5% of compressive strain. Four different frequencies were tested: 0.01, 0.1, 1 and 10 Hz. Preconditioning cycles were required in order to have reproducible measurements (Bergomi et al., 2009): 10 cycles were sufficient for tests performed at 0.1, 1 and 10 Hz, and 3 cycles were enough for tests performed at 0.01 Hz. The zero-displacement was defined for an undeformed HED i.e. inner height of 4 mm (Fig. 2, right).

In summary, 6 bovine coccygeal NP samples were tested at 4 different frequencies, totalizing to 24 experimental runs that were randomly performed. The samples were removed from the fixtures and placed into PBS after each run.

2.4. Water content

The mechanical properties of the NP are highly dependent on its water content (Leahy and Hukins, 2001). It is then important to verify that this parameter does not vary between the different tests performed. Water content of the NP was determined by weighing the sample at harvest, after the mechanical tests, and after drying the sample in the oven at 40 °C for 14 h. The water content is given by

$$\%H_2O = 100 \times \left[1 - \left(M_{dry}/M_{wet}\right)\right] \tag{1}$$

where M_{wet} and M_{dry} are respectively the wet and dry masses of the sample. The water content of the sample is proportional to the volume of the sample, which may change from measurements to measurements. In order to follow these volume changes, a photograph was taken (Vic2D, Limess Gmbh, Germany) at the reference configuration of 2 kPa load (Fig. 2 center up). Assuming a cylindrical shape of the sample, an approximation of the sample relative volume change is given by

$$\Delta V/V = 2\Delta D/D + \Delta H/H \tag{2}$$

where V, D and H are respectively the volume, diameter, and height of the sample for its last mechanical test. The change in diameter ΔD is monitored via the camera (Fig. 2 center) whereas the change in height ΔH is the displacement offset given by the tension machine. Furthermore, the relative volume change directly reflects the relative water content change in the tissue

$$\Delta V/V = \Delta M_{wet}/M_{test} \tag{3}$$

where M_{test} is the wet mass of the sample after testing. Measuring the diameter D_{test}, height H_{test} and mass M_{test} of the samples after testing and combining Eqs. (1) to (3) provides a mean to evaluate the water content change during the experiment

$$\%H_2O = 100 \times \left[1 - \left(M_{dry}/(M_{wet} + \Delta M_{wet})\right)\right]. \tag{4}$$

2.5. Specific damping capacity

There are several metrics that can be used to determine the energy loss in strain–stress data curves. Classically, the dissipation metric is based on the loss angle δ by which strain lags stress. Based on the loss angle, four classes of viscous behaviors can be defined: $\delta = 0$ for perfectly elastic solids, $0 < \delta < \pi/4$ for viscoelastic solids, $\pi/4 < \delta < \pi/2$ for viscoelastic fluids, and $\delta = \pi/2$ for ideal fluids. Although the loss angle can easily be used to classify viscous behaviors of materials, it is not appropriate for energy-based calculations unless an accurate model is introduced. Therefore, the specific damping capacity Ψ defined as the ratio of energy loss over energy input is a more intuitive dissipation metric for this investigation. However, because the NP can show both fluid and solid behaviors (Iatridis et al., 1997), an appropriate energy input metric should be chosen. In this work, following a definition previously proposed (Lee and Hartmann, 1998), we compute the specific damping capacity Ψ as the ratio of ΔW/W, where ΔW is the energy loss per cycle

Fig. 1. (a) and (b) the nucleus pulposus samples are excised using a 7 mm biopsy punch and placed in a PDMS deformable encapsulation device (c). The device is closed with a porous medical grade steel to allow for mass transfer with the sample on one side, and a non porous rigid disc on the other side.

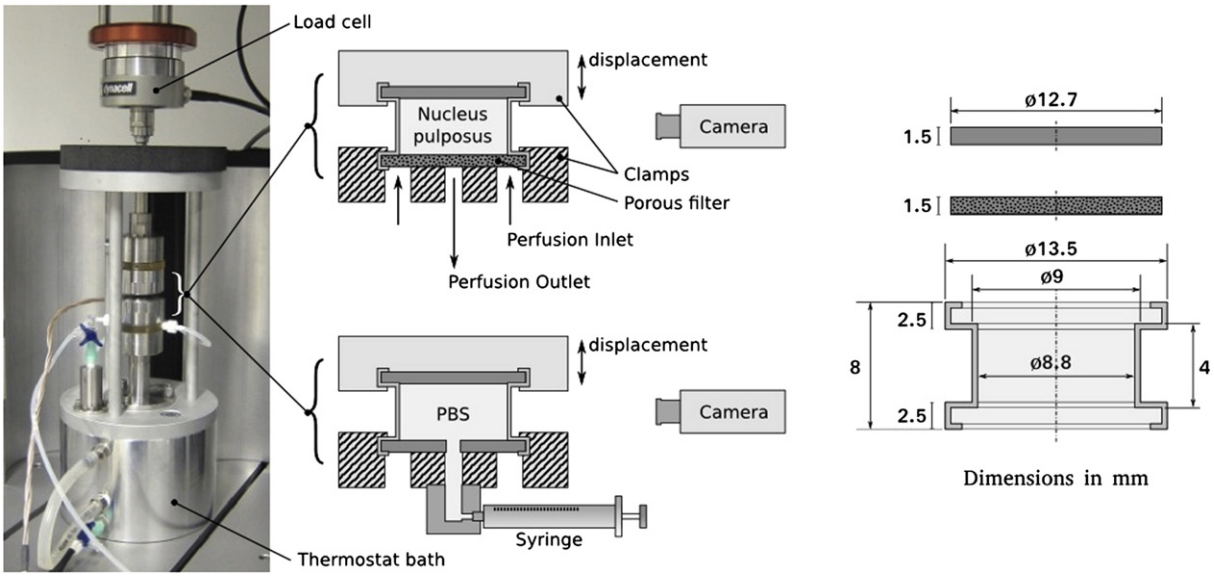

Fig. 2. Mechanical testing system. Left) The encapsulation device is clamped between two special fixtures that allow for perfusion of PBS. Center, up) The sample setup with perfusion. Center, down) The control setup with a syringe controlling the amount of PBS in the encapsulation device. The deformation of the sample is monitored using a camera. Right) Dimension of the encapsulation device.

or hysteresis and W is the work input per cycle. A typical stress–strain curve of one sample and control, as well as their respective hysteresis and work input used in the calculation of the specific damping capacity is given in Fig. 3. This definition presents several advantages that are worth to mention. It is intuitive as it reflects the proportion of energy that is dissipated per cycle; it ranges between nullity and identity, respectively, for perfectly elastic solids and ideal fluids. This metric is thus also appropriate for classification i.e. $\Psi = 0.5$ separates solid and fluid viscoelastic behaviors. Finally, it does not require any modeling assumptions and is most appropriate for non-linear materials.

2.6. Statistical analysis

The HED introduces a systematic error on the quantified mechanical properties of the NP. A paired study using the same HED previously used with the NP sample but filled with PBS was then performed (Fig. 2, center down). Hence, all 24 experimental runs performed on the NP samples were also performed on the chamber filled with PBS only. The same initial configuration was imposed by setting the same displacement offset as measured with the NP runs, and by filling the HED cavity with PBS until a prestress of 2 kPa was reached. As for the NP specimens, two photographs were taken, one at the initial configuration and another at 12.5% strain state for comparison with the corresponding NP sample

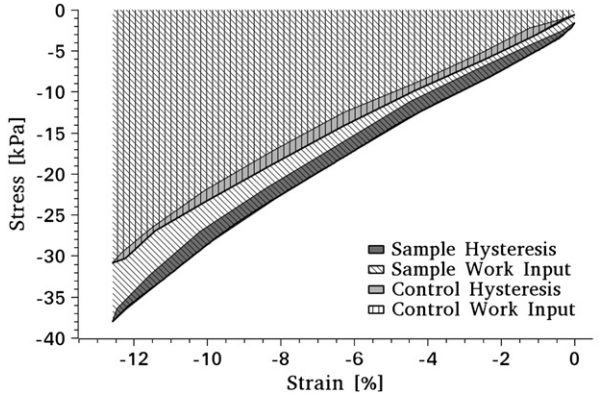

Fig. 3. A typical stress–strain curve of one sample and control, as well as their respective hysteresis and work input used in the calculation of the specific damping capacity.

(Fig. 4). The contribution of the HED on the hysteresis and work input could then be subtracted from the measurements obtained with the NP.

To evaluate if the frequency has an influence on the specific damping capacity, an ANOVA was performed using a statistical significance value of $P<0.05$. Following the ANOVA, a pairwise *t*-test with no adjustment and statistical significance level of $P<0.05$ is used for multiple comparison purposes.

3. Results

3.1. Water content

The NP had an average water content of $\%H2O = 80.6 \pm 3.2\%$ at harvest. Water content significantly increased when encapsulated in the HED. The water content of the samples after testing was $\%H2O = 90.1 \pm 1.6\%$. Throughout 6 h of testing, and according to the water content calculations using Eq. (4), no statistical difference on water content was observed for all the specimens.

3.2. Initial configuration setting

The error of the displacement offset was kept under 20 μm and was considered negligible in respect to the error of the diameter setting. The diameter was controlled by filling the control HED cavity with a 0.01 ml graded syringe until a prestress of 2 kPa was reached. Based on photographs taken at the initial configuration of the paired samples (Fig. 4), the relative diameter error was evaluated to $\Delta D/D = 1.5 \pm 4.0\%$ which, according to Eq. (2), propagates to a relative volume error of $\Delta V/V = 3.0 \pm 8.0\%$. There was no evidence of any statistical correlations between neither hysteresis nor work input of the control and its (inflated) diameter. The effect of the relative diameter error was thus assumed negligible for the calculations of the specific damping capacity.

3.3. Specific damping capacity

The dependency of Ψ on frequency is given in Fig. 5 and Table 1. There is a moderate effect of frequency on the specific damping capacity of the NP ($P = 0.068$). The specific damping capacity at 0.1 and 1 Hz is statistically lower compared to the value at 10 Hz ($P<0.05$) suggesting a minimum of the specific damping capacity Ψ between those frequencies.

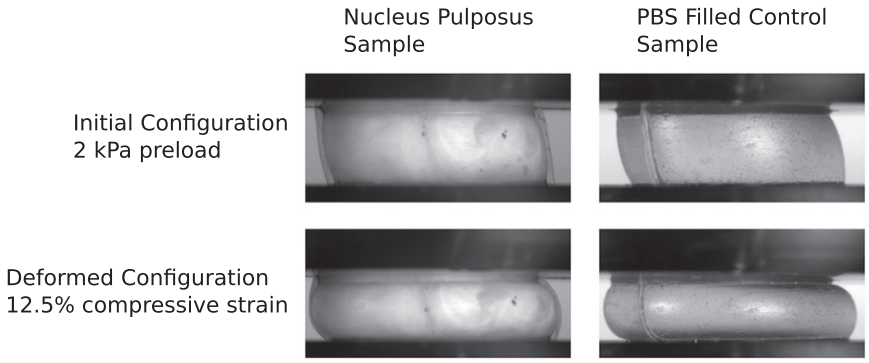

Fig. 4. Images taken to illustrate a paired sample. On the left hand side, the nucleus pulposus is shown (top) at its initial 2 kPa prestress configuration and (bottom) at the deformed 12.5% strain configuration. On the right hand side, the control sample filled with PBS to reproduce the initial configuration of the paired NP sample.

The specific damping capacity at 0.1 Hz has a tendency to be lower compared to the value of 0.01 Hz ($P<0.1$).

4. Discussion

The specific damping capacity of the bovine coccygeal nucleus pulposus was determined for physiological large deformation of 12.5% and for frequencies ranging between 0.01 and 10 Hz. A hydrogel encapsulation device consisting of a PDMS membrane and a porous filter allowed us to obtain a semi-confined situation for the swollen NP samples. This mechanical situation is closer to the way NP naturally works than in tests performed in unconfined or fully confined environments. The semi-confined test provides some mechanical support and geometric definition to the soft tissue, which in turn enables one to analyze its mechanics with relative ease. In particular, the water content of the tissue could be monitored during the experiment, another advantage of the developed technique.

The water content of the NP samples was relatively stable during the experiment, although a 10% increase of water content was measured from harvest. Using a humidity chamber, Iatridis et al. observed a water content loss of $10.0 \pm 4.5\%$ throughout 1 h of shear testing on the human NP (Iatridis et al., 1997). Leahy et al. measured a water content of $81 \pm 2\%$ when testing the sheep NP in cyclic compression; water content stability during testing was not reported in their study (Leahy and Hukins, 2001). It is interesting to observe that although the harvest water content of these studies is equal (approx. 80%), our damping measurements agree, nevertheless, very well to those of Iatridis et al. and Leahy et al. in the range of 1 to 10 Hz and this is despite the fact that some of these studies deviated significantly from harvest water content and in opposite directions. It seems, thus, reasonable to conclude that, although the mechanical properties of the NP depend on water content (Hukins, 1992), damping properties of the NP are not affected between 70 and 90% of water content. This could be verified using the proposed methodology and by using perfusion solutions of various molarities in order to control the extent of NP swelling (Glover et al., 1991).

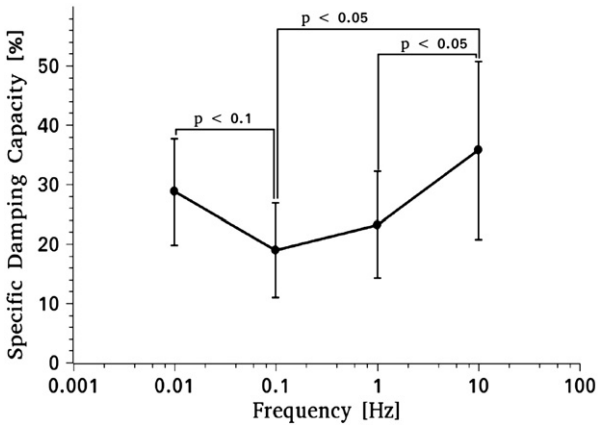

Fig. 5. The specific damping capacity Ψ of the nucleus pulposus is moderately dependent on frequency ($P=0.068<0.1$).

The internal pressure of the HED during deformation is relatively constant and is significantly lower than the pressures found in situ. The order of magnitude of the internal pressure can be estimated using maximum force measurements and the axial surface of the cylindrical HED cavity. At all frequency settings, the maximum pressure was 0.04 MPa. Physiological pressures found in the intervertebral disc are 1 to 2 orders of magnitude higher; intradiscal pressures may range between 0.1 and 2.3 MPa depending on posture and exercise (Wilke et al., 1999). Moreover, the characteristic time constant related to NP consolidation in confined tests is approximately 30 min for a maximum equilibrium stress of 0.06 MPa (Perie et al., 2005). While different than our semi-confined situation, this consolidation time furnished a comparison with the longest cycle period in the present study, which lasted 100 s. It seems then reasonable to assume that hysteresis in the presented measurements was most probably due to viscous phenomena. This explanation is partially supported by our measurements that suggest a minimum value of the specific damping capacity around 0.1 and 1 Hz. We thus hypothesize that there are indeed two competing damping mechanism in the nucleus pulposus. At frequencies lower than 0.1 Hz, damping is probably driven by fluid–solid interactions (poroelasticity), whereas at frequencies higher than 1 Hz, damping is rather driven by solid-solid interactions (viscoelasticity). A detailed analysis of the characteristic timescale for these damping mechanisms could reliably be assessed using spherical indentation techniques (Chan et al., 2012).

This work is consistent with the work of Leahy and Hukins in that damping tends to be lower at values neighboring 0.1 and 1 Hz (Leahy and Hukins, 2001). These frequencies correspond to the dynamics of loads in all day activities such as walking. It must be stressed that the NP is not the only structure that dissipates energy in our back and that due to its relatively low stiffness, the effective damping contribution of the NP in our movements is rather limited. It is nevertheless interesting to observe that for higher frequencies the NP would contribute more to dampen vibration energies of the spine, and that for lower frequencies intrinsic NP fluid flow would be enhanced. This is particularly relevant for tissue-engineered NP replacements as penetration of large-weight

Table 1
The mean specific damping capacity Ψ of the nucleus pulposus at different frequencies. Standard deviations are given in parenthesis, and n is the number of NP samples.

Frequency [Hz]	0.01	0.1	1	10
Ψ [%]	mean 28.7 (SD 9.3)	mean 18.9 (SD 8.2)	mean 23.2 (SD 8.8)	mean 35.7 (SD 15.0)
n	6	6	6	6

solutes is generally attributed to fluid convection rather than diffusion (Ferguson et al., 2004).

Nowadays, hydrogel materials are designed for the replacement of the nucleus pulposus as a solution to manage discogenic pain (Goins et al., 2005). The mechanical specifications of such nucleus replacement devices are still under active investigation. The damping characteristics of the implant have been given relatively small attention and its implication in the biomechanics of the disc and spine remains largely uninvestigated. The present study can then fill a gap in this knowledge.

In conclusion, this work introduces a reliable method to measure the specific damping capacity of soft biological materials in large deformation. Particularly, the specific damping capacity of the coccygeal nucleus pulposus of bovine was measured. In contrast to classical rheology techniques, this method has the advantage to work at the energetic level, which is well suited to study materials in nonlinear regimes.

Conflict of interest

There is no conflict of interest.

Acknowledgments

This project was supported by the Inter-Institutional Center for Translational Biomechanics (EPFL-CHUV-DAL).

References

Adams, M., Bogduk, N., Burton, K., Dolan, P., Freeman, B., 2006. The Biomechanics of Back Pain, 2nd edition. Elsevier Ltd.

Aladin, D.M., Cheung, K.M., Ngan, A.H., Chan, D., Leung, V.Y., Lim, C.T., et al., 2010. Nanostructure of collagen fibrils in human nucleus pulposus and its correlation with macroscale tissue mechanics. J. Orthop. Res. 28, 497–502.

Bergomi, M., Anselm Wiskott, H.W., Botsis, J., Shibata, T., Belser, U.C., 2009. Mechanical response of periodontal ligament: effects of specimen geometry, preconditioning cycles and time lapse. J. Biomech. 42, 2410–2414.

Boxberger, J.I., Orlansky, A.S., Sen, S., Elliott, D.M., 2009. Reduced nucleus pulposus glycosaminoglycan content alters intervertebral disc dynamic viscoelastic mechanics. J. Biomech. 42, 1941–1946.

Chan, E.P., Hu, Y., Johnson, P.M., Suo, Z., Stafford, C.M., 2012. Spherical indentation testing of poroelastic relaxations in thin hydrogel layers. Soft Matter 1492–1498.

Cloyd, J.M., Malhotra, N.R., Weng, L., Chen, W., Mauck, R.L., Elliott, D.M., 2007. Material properties in unconfined compression of human nucleus pulposus, injectable hyaluronic acid-based hydrogels and tissue engineering scaffolds. Eur. Spine J. 16, 1892–1898.

Ferguson, S.J., Ito, K., Nolte, L.P., 2004. Fluid flow and convective transport of solutes within the intervertebral disc. J. Biomech. 37, 213–221.

Glover, M.G., Hargens, A.R., Mahmood, M.M., Gott, S., Brown, M.D., Garfin, S.R., 1991. A new technique for the in vitro measurement of nucleus pulposus swelling pressure. J. Orthop. Res. 9, 61–67.

Goins, M.L., Wimberley, D.W., Yuan, P.S., Fitzhenry, L.N., Vaccaro, A.R., 2005. Nucleus pulposus replacement: an emerging technology. Spine 5, 317S–324S.

Holzapfel, G.A., Schulze-Bauer, C.A., Feigl, G., Regitnig, P., 2005. Single lamellar mechanics of the human lumbar anulus fibrosus. Biomech. Model. Mechanobiol. 3, 125–140.

Hukins, D.W., 1992. A simple model for the function of proteoglycans and collagen in the response to compression of the intervertebral disc. Proc. Biol. Sci. R. Soc. 249, 281–285.

Iatridis, J.C., Setton, L.A., Weidenbaum, M., Mow, V.C., 1997. The viscoelastic behavior of the non-degenerate human lumbar nucleus pulposus in shear. J. Biomech. 30, 1005–1013.

Izambert, O., Mitton, D., Thourot, M., Lavaste, F., 2003. Dynamic stiffness and damping of human intervertebral disc using axial oscillatory displacement under a free mass system. Eur. Spine J. 12, 562–566.

Leahy, J.C., Hukins, D.W., 2001. Viscoelastic properties of the nucleus pulposus of the intervertebral disk in compression. J. Mater. Sci. Mater. Med. 12, 689–692.

Lee, G.F., Hartmann, B., 1998. Specific damping capacity for arbitrary loss angle. J. Sound Vib. 211, 265–272.

Perie, D., Korda, D., Iatridis, J.C., 2005. Confined compression experiments on bovine nucleus pulposus and annulus fibrosus: sensitivity of the experiment in the determination of compressive modulus and hydraulic permeability. J. Biomech. 38, 2164–2171.

Quandieu, P., Pellieux, L., Lienhard, F., Valezy, B., 1983. Effects of the ablation of the nucleus pulposus on the vibrational behavior of the lumbosacral hinge. J. Biomech. 16, 777–784.

Rannou, F., Mayoux-Benhamou, M.-A., Poiraudeau, S., Revel, M., 2004. Anatomy, biology, physiology, and biomechanics of intervertebral disk and other anatomical structures of the lumbar spine. EMC Rhumatol. Orthop. 1, 487–507.

Tsantrizos, A., Ito, K., Aebi, M., Steffen, T., 2005. Internal strains in healthy and degenerated lumbar intervertebral discs. Spine 30, 2129–2137.

Wilke, H.J., Neef, P., Caimi, M., Hoogland, T., Claes, L.E., 1999. New in vivo measurements of pressures in the intervertebral disc in daily life. Spine 24, 755–762.